Lunar and Planetary Science XI

Special Session Abstracts
Eleventh Lunar and Planetary Science Conference
March 17, 1980

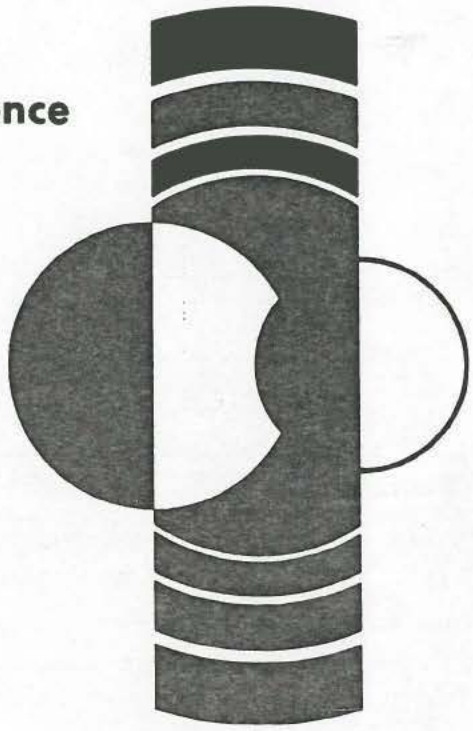

Application of Remote Sensing Techniques to the Study of the Earth

NASA
National Aeronautics and Space Administration

Lyndon B. Johnson Space Center
Houston Texas 77058

LPI/USRA
LUNAR AND PLANETARY INSTITUTE
UNIVERSITIES SPACE RESEARCH ASSOCIATION

APPLICATION OF REMOTE SENSING TECHNIQUES TO THE STUDY OF THE EARTH

SPECIAL SESSION ABSTRACTS
ELEVENTH LUNAR AND PLANETARY SCIENCE CONFERENCE
MARCH 17, 1980

Co-Chaired by

ROGER PHILLIPS AND PITT THOME

Compiled by the
Lunar and Planetary Institute
3303 NASA Road One
Houston, Texas 77058

LPI CONTRIBUTION 399

TABLE OF CONTENTS

STRUCTURAL MAPPING IN TIBET USING LANDSAT IMAGERY

W.S.F. Kidd and Kevin Burke, Department of Geological Sciences, State University of New York at Albany, Albany, NY 12222

Tectonic research on earth during the last fifteen years has been dominated by the need to acquire new information on the plate structure of the lithosphere (1). Satellite derived data have, as yet, contributed relatively little to this work for several reasons: (a) resolution of the earth's gravity and magnetic fields at satellite elevations is too poor to permit discrimination of many plate boundary phenomena; (b) critical plate boundaries commonly lie below sea level and are inaccessible to satellite remote sensing; (c) in some very well known land areas satellite-derived data have little to add to existing structural data (d) some early users of LANDSAT imagery concentrated on mapping linear features indiscriminately (the new basement tectonics) not apparently realizing the importance of separating structures of different ages. The widespread failure of this approach led to the value of LANDSAT imagery as a tool in tectonic studies being seriously underestimated.

It is our experience that LANDSAT imagery can provide an exceptionally powerful tool in structural and tectonic studies in cases where both applicability to specific well-defined scientific problems is appreciated and the limitations of the method are recognized. We have also profited from the peculiar advantages of LANDSAT imagery in studying remote and inaccessible areas. As an example of the use of LANDSAT imagery in structural and tectonic studies we report here on work we have undertaken on the tectonics of the Tibetan (Qinghai-Xizang) plateau.

Terrestrial plate tectonics involves complex, interwoven, cycles of the opening and closing of oceans. Continental collision, marked by the suturing together of two continents, is a particularly significant stage in this sequential process because major structural and compositional changes are achieved within continents at this time. The only places on earth where active collision has reached the stage of complete suturing are in the zone of collision between the Turkish-Iranian plateau and Arabia and in the zone of collision between the Tibetan plateau and India (2).

Three possibilities have been suggested for the elevation of the Tibetan Plateau: (Fig. 1) (A) It may be underlain by crust of normal thickness and is high because beneath it there is anomalous (hot and/or less dense) mantle. (B) It may be underlain by a doubled thickness of continent because India has been thrust below Tibet as Argand suggested (3) or (C) It may be underlain by a doubled thickness of continent because the Asian continent has thickened, concertina-fashion after collision. Fig. 2 is an interpretation of a representative LANDSAT image of central Tibet which seems consistent only with the third possibility. A traverse by Sven Hedin on which rock identifications were made and strikes and dips recorded has been used as ground control.

The LANDSAT images show that rocks on top of the Tibetan Plateau which have yielded Late Cretaceous fossils have almost everywhere been strongly folded and probably thrust indicating substantial N-S shortening (? > 50%). Volcanic rocks are widespread (e.g. on Fig. 2) and are younger than the folding. Our geochemical studies on samples of these volcanic rocks indicate that they are calc-alkaline in character and perhaps result from partial melting of the thickened Asian continent. Studies of old terrains thought to be the sites of ancient continental collisions have shown evidence of substantial shortening and partial melting reminiscent of that seen in Tibet. Elsewhere in Tibet and much of China huge strike-slip faults are seen on

imagery indicating motion of an enormous area toward the Pacific (4) as if escaping from the jaws of the Indian-Asian vise. However, in addition to this faulting, active folding and thrusting in the Tsaidam Basin-Nan Shan region is well displayed on the LANDSAT images. We interpret this area as being in an intermediate stage of development relative to the main Tibetan Plateau, with the shortening and thickening of the crust in progress and the volcanism yet to come. (1) Wilson, J.T. (1965) Nature, v. 207, p. 343-347. (2) Şengör, A.M.C. and Kidd, W.S.F. (1979) Tectonophysics, v. 55 p. 361-376. (3) Argand, E., La Tectonique de l'Asie (1924) C.R. Congr. Geol. Intern. 13 e, 1:171-372. (4) Molnar, P. and Tapponier, P. (1975) Science, v. 189, p. 419-426.

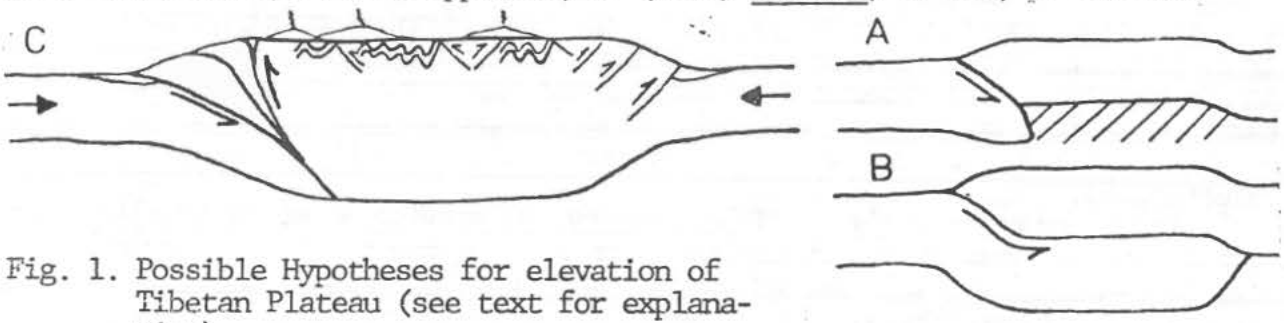

Fig. 1. Possible Hypotheses for elevation of Tibetan Plateau (see text for explanation).

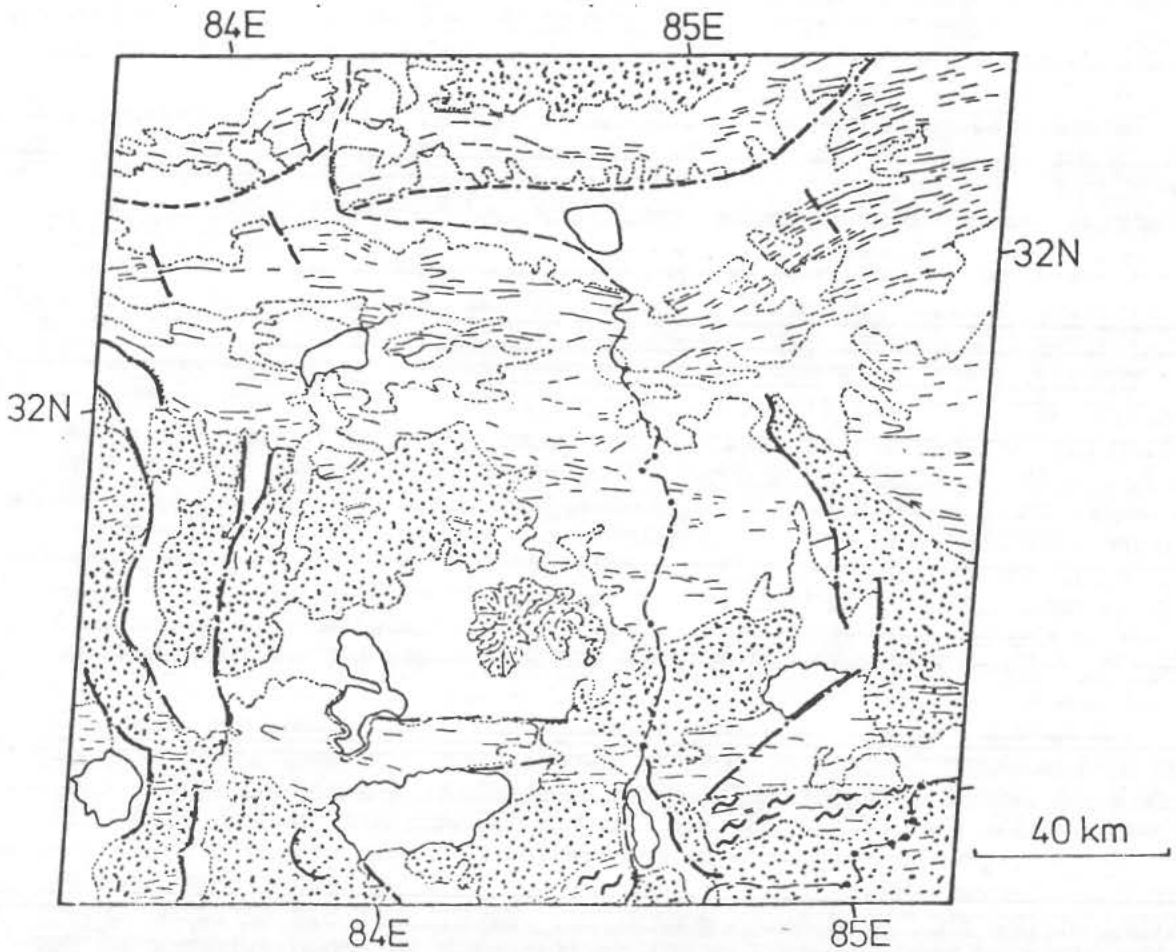

Fig. 2. Geological interpretation of Landsat image #81164-04274-5. White-Lakes and alluvium; dots-volcanics; thin dashes-strike lineaments in Mesozoic limestones and sandstones; ∿ and dashes-pre-Mesozoic phyllites; thick dash-dot lines-faults; dashed lines with few dots-Hedin's traverses with sample points

REMOTE SENSING OF THE EARTH USING MULTISPECTRAL MIDDLE INFRARED SCANNER DATA. Anne B. Kahle, Jet Propulsion Laboratory, California Institute of Technololgy, Pasadena, CA 91103

Laboratory measurements of middle infrared (MIR) (5-40μm) spectra of rocks and minerals show many diagnostic features. The region between 8 and 14μm holds the most promise for remote sensing because this is an excellent atmospheric window and also the region of maximum thermal emission at terrestrial surface temperatures. Within this spectral range, the most prominent spectral features are due to silicon-oxygen stretching vibrations. These change location and intensity with varying composition and structure (Hunt and Salisbury, 1974, 1975, 1976; Lyon, 1965).

The possibility of exploiting these spectral features for remote sensing of rock type from aircraft or satellite has been suggested by many authors (Vickers and Lyon, 1967; Vincent and Thomson, 1972; Vincent, 1975). However, owing to lack of adequate multispectral scanners (Vincent, 1975), very few tests of the technique have been possible. Hovis and others (1968) and Lyon (1972) flew nonimaging spectrometers over areas in California They concluded that even though atmospheric effects were significnt, the reststrahlen bands of silicates were observable. Two tests using a two-channel imaging spectrometer have been reported. Vincent and others (1972) and Vincent and Thomson (1972) flew a scanner having a bandpass between 8.2 and 10.9μm and another bandpass between 9.4 and 12.1μm over a sand quarry near Mill Creek, Oklahoma and over Pisgah Crater, California. By ratioing the spatially registered images, they produced images on which they could distinguish between the quartz sand or sandstone and the nonsilicate surface material at Mill Creek, and at the Pisgah Crater area, were able to distinguish dacite from basalt and rhyolitic tuff from the surrounding alluvium. However, until now the lack of adequate imaging multispectral scanners has precluded further validation of the use of spectral emittance data gathered from aircraft.

Recently we acquired multispectral MIR (8-13μm) scanner data of the East Tintic Mountains in central Utah from the now defunct Bendix 24-channel scanner, flown on the NASA C-130 aircraft. These data consist of six channels of calibrated scanner images of moderate spectral resolution (0.5μm to 1.0μm bandwidth), available in digital format on computer compatible tapes (CCT's). This flight provided an unprecedented opportunity to analyze multispectral MIR image data in a geologically complex area. The district, in an area of high relief and moderate vegetation, consists mainly of Tertiary silicic igneous rocks and Paleozoic quartzite and carbonate rocks that have been locally hydrothermally altered.

The six channels of aircraft data (8.3 - 8.7μm, 8.8 - 9.3μm, 9.4 - 9.9μm, 10.1 - 11.0μm, 11.0 - 12.0μm, and 12.0 - 13.0μm) were contrast enhanced and displayed as black and white images. Because the radiance emitted from the surface is highly dependent upon surface temperature, these images were dominated by temperature (and hence topography). Display of the much more subtle spectral emissivity differences between the channels due to variations in the surface materials required more elaborate image processing.

Using onboard calibration, a simple atmospheric model, and an assumed constant surface emittance of 0.93 in the 11-12μm range, we derived a surface-temperature image from the 11-12μm radiance data. (The 12-13μm data were not used to derive a temperature because of excessive noise.) We could then de-

REMOTE SENSING OF THE EARTH USING MULTISPECTRAL
MIDDLE INFRARED SCANNER DATA

Anne B. Kahle

rive surface-emittance images for the remaining four channels between 8 and 11μm.

Several additional images were prepared from the multispectral radiance and emittance data, including color composites, ratios, color-ratio composites, and principal component transformations. The most satisfactory image product for separation of rock types was produced from the radiance data in channels (8.27-8.7μm), (8.8-9.3μm), and (10.1-11.0μm). The color-enhancement procedure consisted of a nonlinear transformation in which each of the three output channels forming the final color triplet was a function of all three input values. The transformation consists of a principal component rotation, followed by "Gaussian" contrast enhancement and then by an inverse rotation (actually performed by table lookup). This transformation was chosen to remove the correlation that existed between the original components, thus fully utilizing the available color range. A useful feature of the final display is that, although emittance differences appear as variations in color, the intensity of any element of the enhanced scene remains a function of local temperature, just as for the original components. Because temperature is largely topographically controlled, these intensity variations reflect local topography, thus aiding interpretation.

Evaluation of the MIR color composite images was conducted by comparing the distribution of colors in the image with the occurrence of rock units in a generalized lithologic map based on work by Morris, 1964a,b and by field checking critical areas (Kahle & Rowan, 1980). In general, areas shown as red to pink and purple in the image are underlain by rocks in which quartz is a major constituent, whereas blue and green represent rocks that have minor quartz content; green also represents dense vegetation.

The most vivid red areas in the image represent quartzite. Slightly less intense and uniform red areas consist of interbedded sandstone, limestone, quartzite, shale, dolomite and chert. Silicified altered rocks also appear red to pink in the image. Many small red areas correspond to mine dumps and cleared ground around mines, all of which have a high quartz content. The largest exposed mine area, the Dragon mine, is exceptional, however, in that it is purple in the image and has a high clay content (halloysite). Several other areas of argillized rocks have a similar appearance. These differences in color suggest that the red areas indicate the presence of large amounts of quartz, whereas the purple denotes higher proportions of clay minerals.

One of the most surprising contrasts seen in the MIR color-composite image is the separation of quartz latitic-quartz monzonitic rocks from latitic-monzonitic rocks: the former unit appears pink, whereas the latter unit is blue. Important exceptions occur where the rocks are argillized or silicified and, hence, appear purple or red; or where vegetation is dense, in which case the area is green. Calcitic quartz latitic rocks also appear pink, which might be expected because the quartz content was not affected by the alteration process and the calcite has been leached from the surface.

Carbonate rocks generally appear green in the color composite image. However, in some places they are blue or blue-green and therefore similar to the latitic-monzonitic rocks. Preliminary field examination suggests that the blue and blue-green areas correspond to high proportions of sandy soil. Hydrothermal dolomite is compositionally similar to unaltered dolomitic rocks in the study area and, therefore, also appears green and blue-green in the image.

REMOTE SENSING OF THE EARTH USING MULTISPECTRAL MIDDLE INFRARED SCANNER DATA

Anne B. Kahle

The image-processing procedures used to generate the image, although chosen to maximize the differences among surface materials, make it difficult to relate the image color to these spectral differences. However, some general relationships can be noted. Red is consistently related to the presence of quartz-bearing rocks and therefore implies an intense absorption band centered between 8 and 10μm as expected for quartz. In contrast, green appears to represent generally spectrally flat materials such as carbonate rocks and vegetation. In general, the blue correlates with latite and monzonite, both silicate rocks but without quartz as a major constituent.

Examination of spectral-emittance curves derived from the image data suggests that the principal difference we are seeing among the surface materials is in the depth of the spectral features and that variations in the position of the absorption band used in other areas to distinguish among silicate materials (Vincent and Thompson, 1972) appear to be less important here. These results suggest that both intensity and position of the spectral bands need to be studied.

Some distinctions that are not possible in these MIR images can be made in visible and near-infrared (NIR) color-ratio composite images that were previously produced from NASA 24-channel scanner data specifically for mapping hydrothermally altered rocks and vegetation distribution. Although both carbonate rocks and vegetation lack significant absorption bands in the 8-12μm region, the fact that they are readily distinguishable in the visible and NIR color-ratio composite images allows mapping of the carbonate rocks. Argillized rocks and quartz latitic rocks are not consistently distinguishable in the MIR image, but are clearly separable in the visible and NIR image owing to their spectral contrast in the 2.2μm region. Thus, use of color-composite images from both the MIR and the visible and NIR, combined with limited field checking, permit mapping of quartzite, carbonate rocks, quartz latitic and quartz monzonitic rocks, latitic and monzonitic rocks, silicified altered rocks, and argillized altered rocks.

Hovis, W. A., Jr., L. R. Blaine and W. R. Callahan, Appl. Optics, 7, 1137-1140, 1968. Hunt, G. R. and J. W. Salisbury, Air Force Cambridge Research Lab., AFCRL-TR-74-0625, 1974, AFCRL-TR-75-0356, 1975, AFCRL-TR-76-0003, 1976. Kahle, A. B., D. P. Madura and J. M. Soha, Jet Propulsion Lab. Publ. 79-89, 1979. Kahle, A. B. and L. C. Rowan, to be published in Geology, May, 1980. Lyon, R. J. P., Science, 175, 983-986, 1972. Morris, H. T., U. S. Geological Survey Bull., 1142-K, 29 p., 1964a, 1142-L, 1964b. Vickers, R. S. and R. J. P. Lyon, pp. 585-607, Thermophysics of Spacecraft and Planetary Bodies, G. B. Heller, Ed., Academic Press, Inc., New York, 1967. Vincent, R. K, Proc. IEEE, 63, 137-147, 1975. Vincent, R. K. and F. Thomson, J. Geophys. Res., 77, 2465-2472, 1972. Vincent R. K., F. Thomson and K. Watson, J. Geophys. Res., 77, 2473-2477, 1972. Vincent, R. K., L. C. Rowan, R. E. Gillespie and C. Knapp, Remote Sensing of Environment, 4, 199-209, 1975.

REMOTE ANALYSIS OF MICRO-RELIEF ON NATURAL TERRAIN: THE POTENTIAL OF IMAGING AND NON-IMAGING RADAR, Gerald G. Schaber, U.S. Geological Survey, Flagstaff, AZ; Graydon L. Berlin, Northern Arizona University, Flagstaff, AZ; Walter E. Brown, Jet Propulsion Laboratory, Pasadena, CA; and Steve C. Reid, Lockheed Electronics Company, Inc., Houston, TX.

The geologic potential of side-looking radar image data (airborne and spacecraft-borne) can be divided into two major categories; first, the photo-like presentation which emphasizes gross morphology and tectonic structures; second, the backscatter function, related to normalized radar cross-section (σ_0) versus surface parameters (dominantly small scale relief) at specific angles of radar illumination. The radar image is actually a two dimensional plot of radar reflectivity consisting of a large number of resolution cells, each of which represents the value of σ_0 for a specific portion of the image area or terrain. This image represents the "actual" distribution of radar reflectance from the terrain *only* if the relations between film density (grey level) of each resolution element and corresponding actual σ_0 value are known; as well as the relative terrain location or geometric position of each resolution element. A radar image then actually records a *statistical sampling* of fluctuating reflection signals. Conceptually, radar images are related to σ_0 so that lighter tones (on the image) generally represent higher decibel values of σ_0, while darker tones represent lower σ_0 values. *Evaluation of side-looking airborne and spacecraft (Seasat) radar images for quantitative roughness information has been severely restricted because of the lack of these calibrations.*

Direct measurement of *calibrated* backscatter power, as a function of incidence angle of illumination, can be obtained from a radar *"scatterometer"*, a non-imaging radar system designed to measure σ_0 from radar reflectivity time-histories as a function of θ_i (incidence angle) at a particular wavelength and polarization. Surface relief statistics have been insufficiently known at millimeter-to-meter scale over large, flat and homogeneous regions of natural terrain to fully test theoretical backscatter models or to derive empirical scatter models that correctly predict terrain relief statistics.

We have recently completed a major investigation of radar backscatter in Death Valley, CA. involving correlation of millimeter-to-meter scale relief statistics with radar image and radar scatterometer data sets for nine saltpan and gravel surfaces. A technique was developed to analyze high resolution surface profiles into over one hundred separate statistical parameters of relief, power spectra, slope and curvature using terrain analysis software developed for other purposes by the U.S. Geological Survey over the past one and one-half decades (1). These terrain statistics have been correlated with "relative" return power as recorded on radar image data (including Seasat) and "absolute" values of σ_0 derived from analysis of radar scatterometer time-histories. We have previously showed that a sharp flexure in the backscatter function of L-band (25-cm wavelength) radar image data of Death Valley saltpan and gravel surfaces can be related to onset of the Rayleigh scattering regime (2). More recent reports in the Death Valley series describe the excellent qualitative discrimination of geologic units using multifrequency, multi-polarization radar, Landsat multispectral scanner images, and various combinations of these data sets (3,4).

A modified version of the Bragg-Rice radar backscatter model has been developed and has been calibrated using the detailed measurements of micro-relief in Death Valley. The radar parameters wavelength, polarization, incidence angle and radar cross-section are related via this model to the surface

parameters surface height deviation, the shape of the surface height spectrum, and the effective complex dielectric constant. The radar cross-section data used to establish the algorithm calibration was obtained by the Johnson Space Center four-frequency scatterometer.

In order to test the validity of the Death Valley backscatter algorithms on completely different terrain types, we have initiated in recent months a new study of radar image (including Seasat) and scatterometer data obtained over a diverse volcanic and sedimentary test site in the high desert plains of northern Arizona. Radar image data sets are rather extensive for this test site and include recently obtained dual frequency, dual polarization (and incidence angle), synthetic aperture images in mapping (overlap) format.

Multifrequency airborne radar image data of SP Mountain and SP flow (and vicinity) in north-central Arizona were obtained in diverse viewing directions and direct and cross-polarization, then compared with surface and aerial photography , LANDSAT multispectral scanner data, airborne thermal infrared imagery, surface geology, and surface roughness statistics (5). The extremely blocky, basaltic andesite of SP flow is significantly brighter on direct-polarization K-band (0.9-cm wavelength) images than on cross-polarized images taken simultaneously. Conversely, for the longer wavelength (25 cm) L-band radar images, the cross-polarization image returns from SP flow are brighter than the direct-polarized image. This effect is explained by multiple scattering and the strong wavelength dependence of polarization effects caused by the rectilinear basaltic andesite scatters. Two distinct types of surface relief on SP flow, one extremely blocky, the other subdued, are found to be clearly discriminated on the visible and thermal wavelength images but are separable only on the longer wavelength L-band radar image data. The inability of the K- and X- (3-cm wavelength) band radars to portray the differences in roughness between the two SP flow surface units is attributed to the radar frequency dependence of the surface-relief scale, which, described as the Rayleigh criterion, represents the transition between quasispecular and primarily diffuse backscatter.

This research represents one phase of radar studies carried out at the U.S. Geological Survey under National Aeronautics and Space Administration contract W13,709 and at the Jet Propulsion Laboratory (California Institute of Technology) under NASA contract NASA 7-100.

REFERENCES

(1) Schaber, G., Pike, R., and Berlin, G. (1979) Terrain-analysis procedures for modeling radar backscatter: U.S. Geol. Survey Open-File Rept. 79-1088, 67 p.

(2) Schaber, G., Berlin, G., and Brown, Jr., W. (1976) Variations in surface roughness within Death Valley, CA: Geologic evaluation of 25-cm wavelength radar images: Geol. Soc. Am. Bull., 87, 29-41.

(3) Dailey, M., Elachi, C., Farr, T., and Schaber, G. (1978) Discrimination of geologic units within Death Valley using multifrequency and multipolarization imaging radar data: Geophys. Res. Lett., 5, 889-892.

(4) Dailey, M., Elachi, C., Farr, T., Stromberg, W., Williams, S., and Schaber, G. (1978) Applications of multispectral radar and Landsat imagery to geologic mapping in Death Valley: Jet Prop. Lab. Pub. 78-19, 47 p.

(5) Schaber, G., Elachi, C., and Farr, T. (1980) Remote sensing data of SP Mountain and SP lava flow in North-Central Arizona: Remote Sensing of Environment, 9(2), 149-170.

OBSERVATION OF SAND DUNES USING SPACEBORNE IMAGING RADAR.

C. Elachi and R. Blom, Jet Propulsion Laboratory, Pasadena, CA 91103

Since aeolian processes are responsible for much arid land geomorphology and since they are indicators of both past and present climatic conditions, they are of considerable importance to Earth and planetary studies. Much of the interest in Mars has centered around aeolian activity (1-5). Should similar aeolian features exist on Venus, it is important that any radar imaging system sent to explore Venus have the capability of detecting them. In order to understand the capability of spaceborne imaging radar to image and characterize sand dunes, and to understand the imaging mechanisms, a study was undertaken using the Seasat SAR images of a number of sand dune fields in the southwestern United States (Algodones, Mohawk, Kelso and Cadiz dunes) and northwestern Mexico (Sonora dunes).

The broad synoptic view provided by spaceborne imaging systems has proven valuable in the global study of sand dunes on the Earth (6-8). The Landsat and Skylab images used in these studies provide a benchmark with which to compare the orbital radar images for evaluation. The radar images were obtained with the Seasat-A SAR (Synthetic Aperture Radar), which had the following parameters: L-band frequency, 24cm wavelength, horizontal polarization, $20^{o} \pm 3^{o}$ incidence angle (from vertical), 100km imaging swath, and a radar resolution of about 25 meters. The satellite was in a near polar orbit (108^{o} inclination), at an altitude of 790km. Two illumination directions were possible in the region of study: $N72^{o}$ E during the ascending pass and $N72^{o}$ W during the descending pass.

Figure 1 shows the Landsat and Seasat SAR images of the Algodones dunes in southeast California. Large scale aeolian features in the main dune field include parallel dunes on the west side, complex coalesced domical dunes in the west center of the dune field and giant crescent dunes from the central portions to the southeastern end of the chain. Also note the central ridge which runs down along the axis of the field from the north to the central portion of the dunes. The intradune flats separating the crecentic dunes are exposed alluvial substrate with less than 10cm relief (9).

The Seasat SAR images show all the various aeolian features seen on Landsat. The dunes are observed as characteristic variations in the image tone, particularly the density of bright points. Upon comparing the two radar images it is clear that from a certain illumination direction the radar images mostly the dunes with facets perpendicular to the illumination direction. In Figure 1b, the high central ridge shows as a bright band followed by a dark band. The dark band corresponds to the region which is sloping away from the radar with a slope of about 7^{o} leading to a local incidence angle of about 30^{o} from vertical.

These observations, and similar ones for the other dune fields, led to the conclusion that the dunes are imaged because of the specular return from appropriately oriented facets. Field measurements by Sharp (10) in the Kelso dunes showed that sand ripples have heights between 0.5 and 1cm, and wavelengths between 7.5 and 18cm. If we consider the radar roughness criterium, a surface would look smooth if the rms height is less than

$$h_s = \lambda / 8 \cos\varphi$$

where φ = incidence angle. In the case of Seasat, h_s = 2cm even when the surface has a slope of 30^{o} away from the radar. If we consider the Bragg scattering effect, the Bragg wavelength is

$$\Lambda = \lambda / 2 \sin\varphi$$

and Λ is always larger than 17cm even for slopes of $+30^{o}$ away from the radar. Thus it seems that sand dunes do indeed act as perfectly flat surfaces and the radar return is dominated by specular return.

This has some major implications on the radar capability to image sand dunes. Because sand dunes' facets will always have a slope less than 33^{o}, the imaging radar must have an incidence angle of less than 33^{o} to be able to image them. Also the radar will be able to best image the dunes with facets oriented almost toward the radar. Therefore it is important to have at least two illumination directions.

These conclusions are also consistent with the observations of the sand dunes studied and with airborne radar observations at multiple incidence angles and look directions. (1) Breed, C.S., (1977) Icarus, p. 326-340. (2) Cutts, J.A. and Smith, R.S.U., (1973) Jour. Geophy. Res., p. 4139-4154. (3) McCauley, J.F., (1973) Jour. Geophy. Res., p. 4123-4137. (4) Sagan, C., et al., (1971) Icarus, p. 253. (5) Sagan, C., et al. (1972) Icarus, p. 346. (6) McKee, E.O. and Breed, C.S., (1976) U.S.G.S. Prof. Paper 929, p. 81-88. (7) Breed, C.S., et al. (1979) U.S.G.S. Prof. Paper 1052, p. 305-421. (8) Breed, C.S. and Grow, T. (1979) U.S.G.S. Prof. Paper 1052, p. 253-302. (9) Sharp, R.P., (1979) Geol. Soc. Amer. Bull. p. 908-916. (10) Sharp, R.P., (1963) Jour. Geol. p. 617-636.

RADAR OBSERVATION OF SAND DUNES

ELACHI, C., et al.

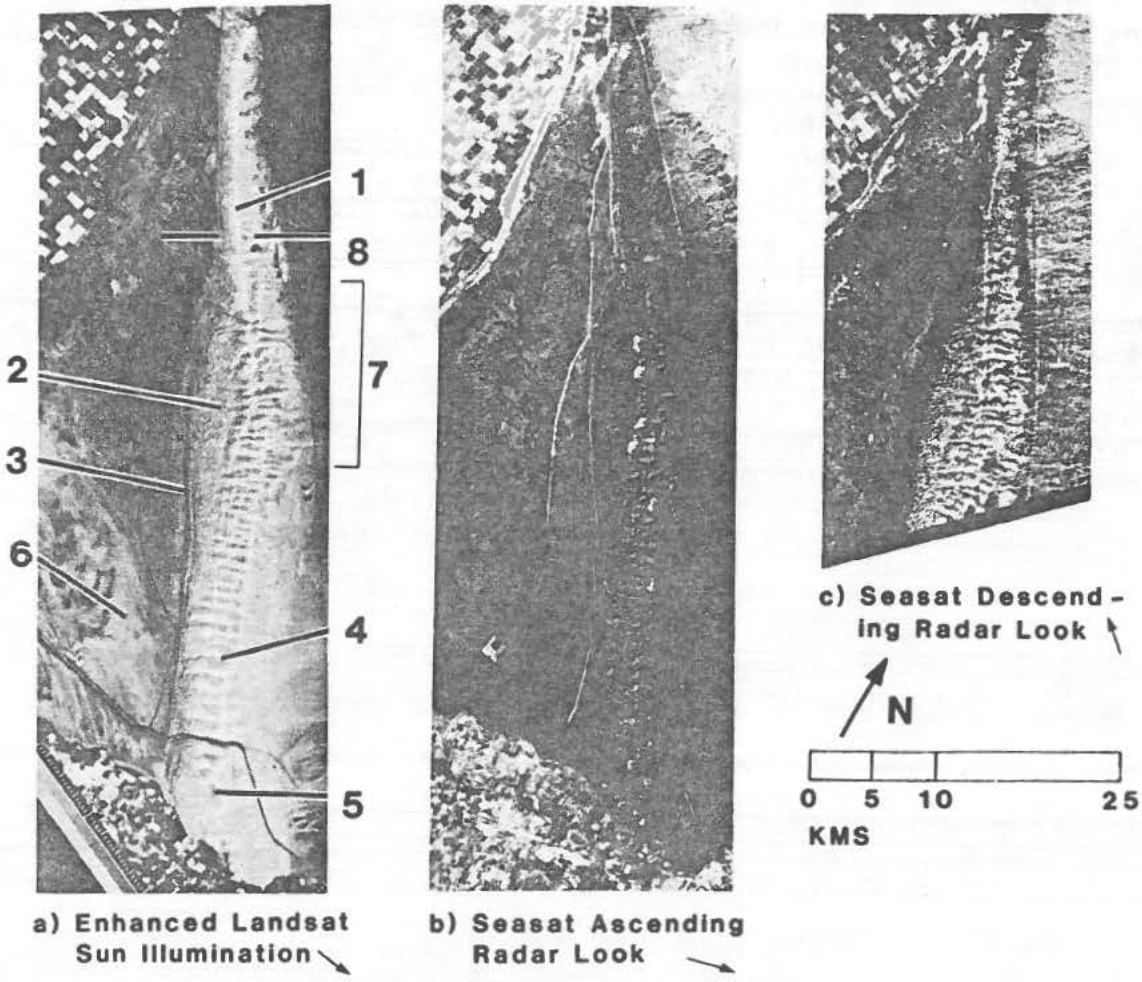

ORBITAL IMAGERY OF ALGODONES DUNES

Features noted on Landsat image are: 1. Axial Ridge 2. Domical Dunes 3. Linear Dunes 4. Crescentic Dunes 5. Location of small Barchans 6. Sand Sheets and Stringers.

LARGE SCALE VARIATIONS IN THE MAGNETIZATION OF THE EARTH'S CRUST. R.A. Langel, Geophysics Branch, NASA Goddard Space Flight Center, Greenbelt, MD 20771

In a pioneering effort, Regan et al. (1) showed that it was possible to detect and map very long wavelength magnetic anomalies with satellite data from the Polar Orbiting Geophysical Observatory (POGO) satellites. Their map contained striping along the orbit path due to pass-to-pass level differences from varying external fields. Mayhew (2) developed a technique to remove these level differences and Langel (3) used Mayhew's techniques to produce a revised map. At high latitudes, fields of ionospheric origin cause severe problems in isolating the anomaly fields. Langel et al. (4) derived an anomaly map from POGO data for western Canada and compared it with upward continued aeromagnetic data. The agreement was very good, confirming not only our ability to isolate the anomaly fields, but also the reality and crustal origin of the anomaly fields derived from satellite data. In view of these results, we have now derived the anomaly maps for the high latitudes of both hemispheres shown in Figures 1 and 2.

For interpretation it is necessary to convert the anomaly maps to a model of crustal magnetization. Because we have only scalar data, the assumption is made that the magnetization is parallel to the ambient field. Orthogonal components of magnetization would be transparent to this data. As a first step we assume a constant thickness magnetic crust with laterally varying magnetization and calculate the magnetization which would give rise to the measured anomalies. This calculation also yields the capability of reducing the data to common altitude and inclination. Such a relative magnetization map for the U.S. is shown in Figure 3. Some known geologic features are readily apparent on the map: the Colorado Plateau, Basin and Range, Rio Grande Rift, Mississippi Embayment, Michigan Basin, etc. The next step is to choose a localized feature and make a more realistic and detailed model, adding the constraints of correlative data such as gravity anomalies, refraction profiles, heat flow, aeromagnetics, etc. A preliminary version of such a model has been derived for the major magnetic anomaly in Kentucky.

(1) Regan et al. (1975) JGR, p. 794-802. (2) Mayhew (1979) Jour. of Geophysics, p. 119-128. (3) Langel (1979) EOS, p. 667. (4) Langel et al. (1979) NASA TM 80568, submitted to Can. J. of Earth Sciences.

CRUSTAL MAGNETIZATION

Langel, R.A.

NORTH POLAR ANOMALIES IN SCALAR MAGNETIC FIELD FROM THE POGO SATELLITES

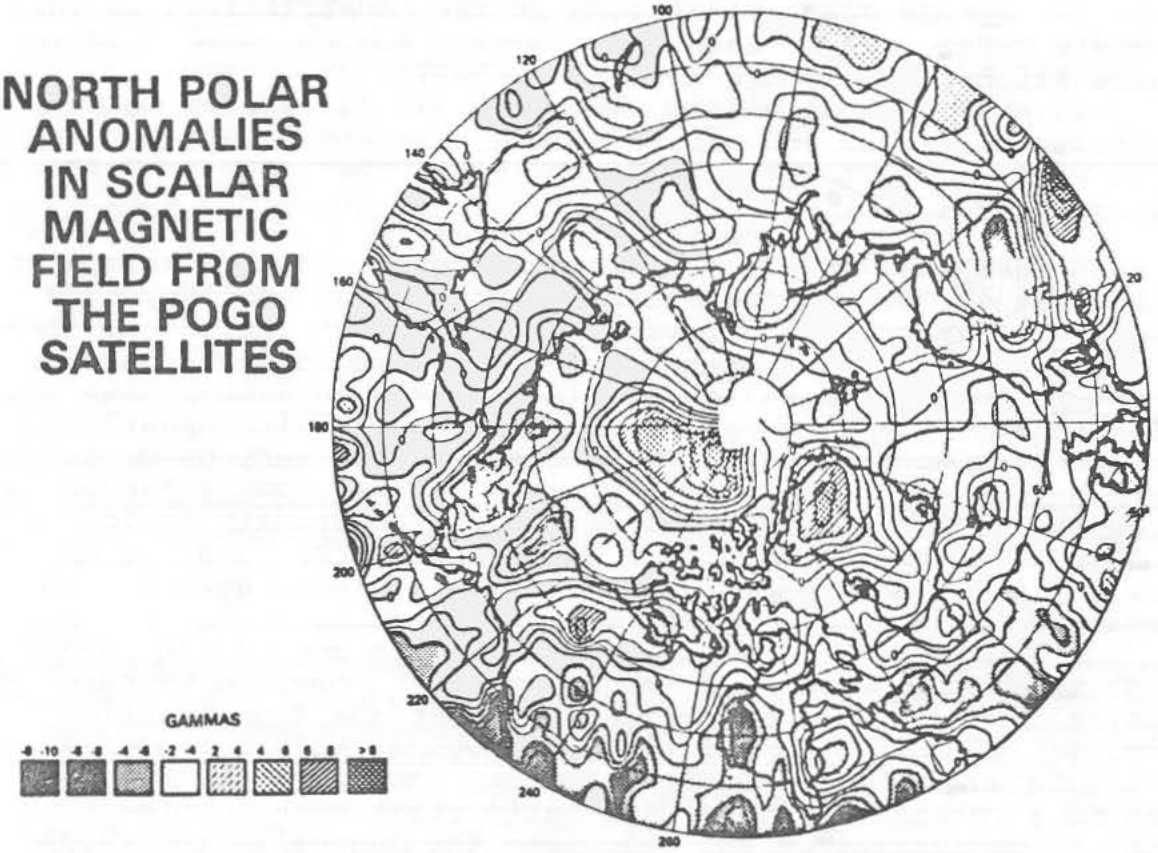

SOUTH POLAR ANOMALIES IN SCALAR MAGNETIC FIELD FROM THE POGO SATELLITES

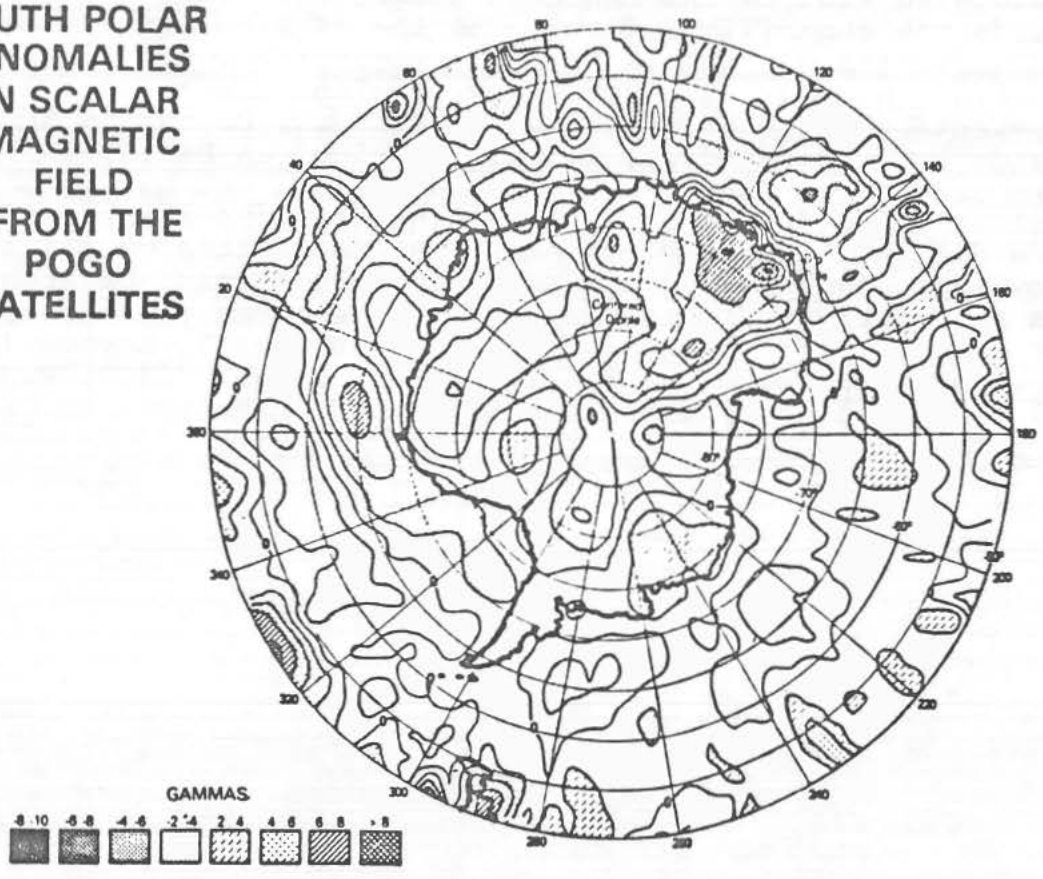

CRUSTAL MAGNETIZATION

Langel, R.A.

EQUIVALENT BULK MAGNETIZATION DERIVED FROM POGO SATELLITE DATA ASSUMING A CONSTANT THICKNESS MAGNETIC CRUST OF 40 KM. UNITS ARE EMU/CC x 10^4.

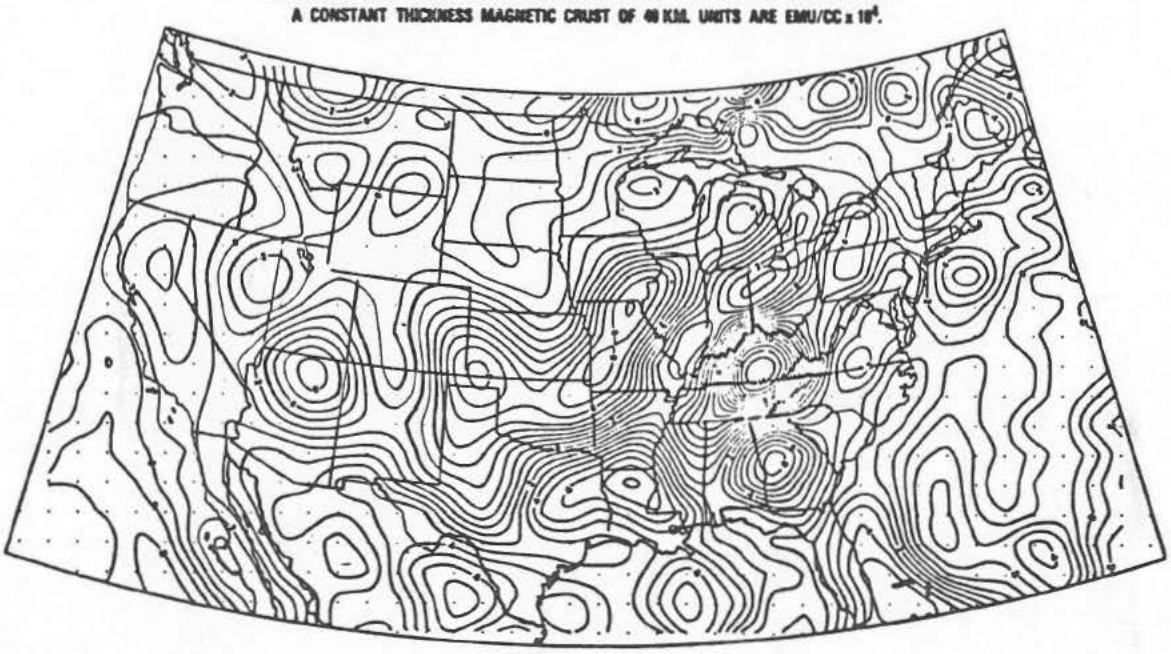

UNIVERSITIES SPACE RESEARCH ASSOCIATION

THE LUNAR AND PLANETARY INSTITUTE

MEMORANDUM

DATE: 26 February 1980

TO: Paula Robertson

FROM: Fran Waranius FBW

SUBJECT:

The following paper has been assigned Lunar and Planetary Institute Contribution No. 399

APPLICATION OF REMOTE SENSING TECHNIQUES TO THE STUDY OF THE EARTH
Special session abstracts 11th Lunar & Planetary Science Conference
Co-Chaired by Roger Phillips and Pitt Thome

Will you please insert this number on your galleys or page proofs before final submission to publisher.

When you send us the reprint order form, please indicate the NUMBER OF PAGES in the galley. We need this information to compute costs on our purchase order. If you receive any information concerning page charges, please forward this to us, as well.

Thank you for your help.

* Please be sure print order includes at least 50 copies for L/IC Distribution purposes.

Thank you.